

Article

# An Important Factor Affecting the UV Aging Resistance of PBO Fiber Foped with Nano-TiO<sub>2</sub>: The Number of Amorphous Regions

Jiping Liu <sup>1,2,\*</sup>, Xiaobo Liu <sup>1,2</sup>, Dong Wang <sup>1</sup> and Hu Wang <sup>1</sup>

<sup>1</sup> School of Materials Science and Engineering, Beijing Institute of Technology, Beijing 100081, China; liuxiaobo0425@126.com (X.L.); wd2263988@163.com (D.W.); wanghu123@bit.edu.cn (H.W.)

<sup>2</sup> State Key Laboratory of Explosion Science and Technology, Beijing 100081, China

\* Correspondence: liujp@bit.edu.cn

Received: 14 February 2019; Accepted: 11 May 2019; Published: 13 May 2019



**Abstract:** Modified nano-TiO<sub>2</sub> was prepared by using triethanolamine and tetraisopropyl di (dioctylphosphate) titanate, respectively. Then the poly(p-phenylene benzobisoxazole) (PBO) fibers doped with different additions of modified nano-TiO<sub>2</sub> particles were prepared by preparing PBO polymer solution and dry-jet wet spinning technique. Thermogravimetric and derivative thermogravimetry results showed that the addition of nano-TiO<sub>2</sub> could improve the crystallinity and maximum thermal decomposition rate temperature of PBO fibers. Tensile strength results showed that nano-TiO<sub>2</sub> addition did not affect the tensile properties of PBO fibers before ultraviolet (UV) aging began, and nano-TiO<sub>2</sub> with addition values lower than 3% could improve the UV aging resistance performance of PBO fibers, while the aging resistance would be seriously reduced if values were over 5%. The size and quantity of the amorphous regions have a more important influence on the aging resistance of PBO fibers.

**Keywords:** titanium dioxide; poly(p-phenylene benzobisoxazole); ultraviolet aging; amorphous region

## 1. Introduction

Poly(p-phenylene benzobisoxazole) (PBO) fiber, a kind of rigid-rod isotropic crystal polymer, has excellent thermal stability, solvent resistance, remarkable tensile strength, and modulus [1–3]. PBO fiber known as a sort of synthesis material has become prominent in high strength applications, such as body armor, ropes and cables, and recreational equipment [4]. However, the ultraviolet (UV) aging resistance performance of PBO is poor. UV light irradiation was a frequently encountered factor that could induce photo-degradation of polymers in the outdoor environment [5,6]. PBO fiber was sensitive to UV light exposure, which could cause chemical, physical and mechanical properties changes.

Many studies have attempted to improve the aging resistance of PBO fiber [7–10]. Among them, introducing anti-ultraviolet agents received a great deal of attention [11–13]. As a strong UV absorber, nano-TiO<sub>2</sub> has perfect versatility in optical, electrical, and photochemical properties [14–17], and can improve the resistance to UV aging of PBO fiber [18]. Many methods have been explored to prepare the nano-TiO<sub>2</sub>/PBO nanocomposites, such as sol–gel blending technique [19], in situ polymerization process [20,21] and solution blending [22]. However, nano-TiO<sub>2</sub> has extremely large surface energy and is not easily dispersed in fiber matrix [23]. Meanwhile, the compatibility of PBO fibers with titanium dioxide particles is poor, and cracks and defects are easily produced at the interface between them. Therefore, achieving the compatibility between nano-TiO<sub>2</sub> and PBO matrix and achieving uniform dispersion of nano-TiO<sub>2</sub> in PBO matrix are the key problems.

To solve this problem, we used triethanolamine (TEA) and tetraisopropyl di (dioctylphosphate) titanate (TDT) to prepare modified nano-TiO<sub>2</sub> via surface modification which can help to form chemical and physical interactions between two incompatible phases [12,24–26]. Then the modified PBO fiber with different TiO<sub>2</sub> contents was synthesized using typical PBO polymerization conditions.

The characterization of modified nano-TiO<sub>2</sub> and its effect on the properties of PBO fiber were determined in this study. Thermogravimetric (TG) and derivative thermogravimetry (DTG) were used to determine the thermal properties of modified nano-TiO<sub>2</sub> and modified PBO fiber. The element contents of modified nano-TiO<sub>2</sub> samples were determined by X-ray fluorescence (XRF). Furthermore, the microstructure of nanoparticles and fiber were evaluated via scanning electron microscopy (SEM) characterization of the surface morphology. In addition, Fourier transform infrared (FTIR) spectroscopy was used to further investigate the compositional changes of nano-TiO<sub>2</sub> and PBO fiber. In addition, a schematic diagram of the influence mechanism of the size and quantity of crystal region on the aging resistance performance of PBO fiber was provided.

## 2. Experimental Procedure

### 2.1. Preparation of Modified Nano-TiO<sub>2</sub>

The modified nano-TiO<sub>2</sub> was prepared by surface modifying nano-TiO<sub>2</sub> (99.9% purity, average particle size: 50 nm, mainly composed of rutile phase, Sinopharm Chemical Reagent Beijing Co., Ltd., Beijing, China) with TEA (99.7% purity, Sinopharm Chemical Reagent Beijing Co., Ltd., Beijing, China) and TDT (99.7% purity, Sinopharm Chemical Reagent Beijing Co., Ltd., Beijing, China), respectively. A certain number of nano-TiO<sub>2</sub> particles in 65% TEA aqueous solution was first treated in an ultrasonic bath (frequency of 40 kHz, power 300W, GT SONIC, Guangdong, China) for 30 min, and then stirred for 2 h with reflux at 90 °C. Then the treated nano-TiO<sub>2</sub> particles were filtered and dried at 100 °C for 6 h in a vacuum system. Subsequently, the treated nano-TiO<sub>2</sub> particles were modified with TDT at 100 °C and on the pH value of 3.6 for 2 h according to the weight ratio of nano-TiO<sub>2</sub>, TDT, water, and isopropanol to 4:2:95:3. The modified nano-TiO<sub>2</sub> particles were filtered and washed with distilled water three times and washed with ethanol one time and dried at 100 °C for 6 h in a vacuum system to remove the solvent. The procedure of preparing surface-modified nano-TiO<sub>2</sub> is shown in Figure 1.

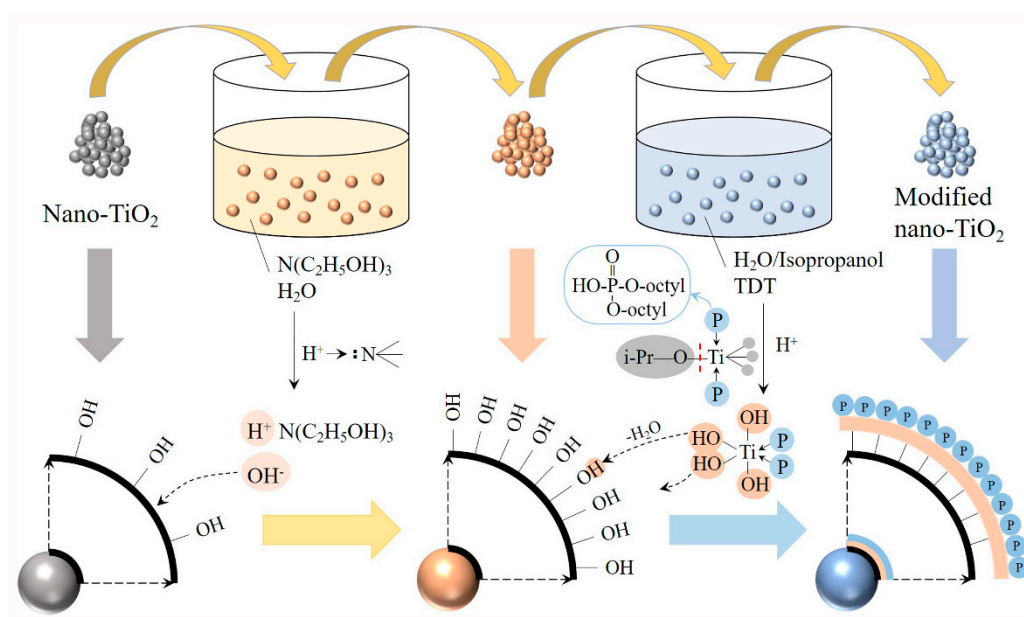
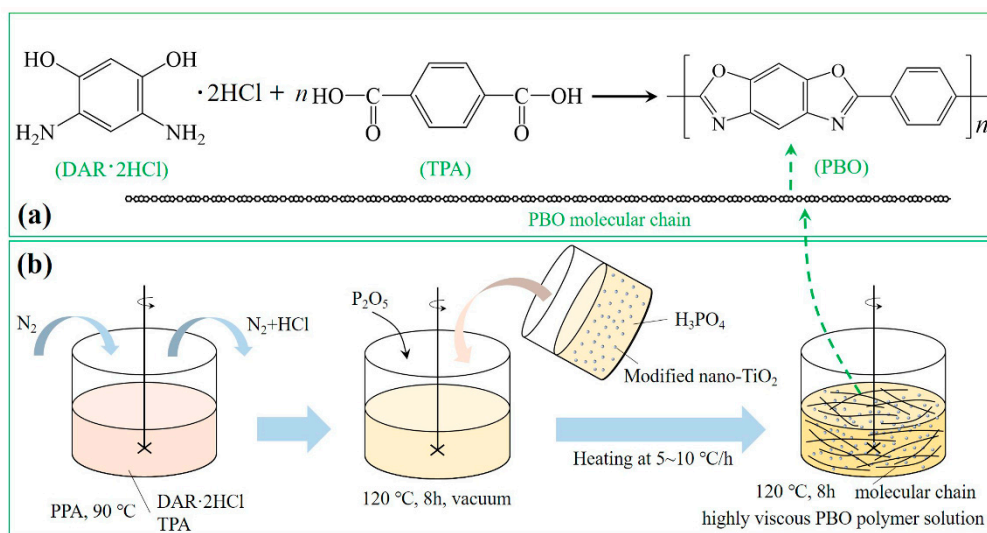


Figure 1. Procedure of preparing surface-modified nano-TiO<sub>2</sub> particles.

## 2.2. Preparation of PBO Fibers

The PBO fibers doped with different additions of modified nano-TiO<sub>2</sub> particles were prepared as follows.

The PBO polymer solution was prepared by using the polycondensation of 4,6-diaminoresorcinol dihydrochloride (DAR·2HCl, 99.9% purity) and terephthalic acid (TPA, 99.9% purity, dried before use) doped with different additions (0%, 1%, 3%, 5%) of modified nano-TiO<sub>2</sub> particles [27,28]. The poly (phosphoric acid) (PPA, with a phosphorus pentoxide content of 70.7 wt %) was loaded into a glass vessel equipped with a mechanical stirrer and nitrogen inlet/outlet. Then DAR·2HCl and TPA were placed in PPA and mixed together with PPA at 90 °C under a nitrogen (N<sub>2</sub>) atmosphere until complete removal of hydrochloride (HCl). The mole ratio of DAR·2HCl and TPA was 1:1. Modified nano-TiO<sub>2</sub> particles which were placed in phosphoric acid (H<sub>3</sub>PO<sub>4</sub>) and treated with ultrasonic bath (40 kHz) for 30 min were added to the glass vessel. Phosphorus pentoxide (P<sub>2</sub>O<sub>5</sub>) was then added to the glass vessel to ensure the P<sub>2</sub>O<sub>5</sub> concentration up to 85% and result in a final polymer concentration of 14%. The polymerizing mixture was first stirred under vacuum at 120 °C for 8 h and then heated to 180 °C stepwise at 5–10 °C per hour and kept at 180 °C for another 8 h with constant stirring. Then a highly viscous PBO polymer solution doped with nano-TiO<sub>2</sub> particles was prepared (see Figure 2b). By changing the amount of modified nano-TiO<sub>2</sub>, we prepared four kinds of fibers with modified nano-TiO<sub>2</sub> content of 0%, 1%, 3%, 5%, respectively. The scheme of PBO preparation was shown in Figure 2a and the procedure of preparing a PBO polymer solution was shown in Figure 2b.



**Figure 2.** Scheme of PBO preparation (a), and procedure of preparing poly(p-phenylene benzobisoxazole) (PBO) polymer solution (b).

The obtained highly viscous PBO polymer solutions in PPA were then spun into PBO fibers using dry-jet wet spinning. The fiber exited into a 10 cm long air gap before entering a distilled water coagulation bath maintained at room temperature. Draw ratios as high as 10 were achieved. Fibers were wound on a plastic spool, washed in running water for a week, and subsequently dried overnight in a vacuum at 80 °C. The procedure of dry-jet wet spinning of PBO fibers is shown in Figure 3.

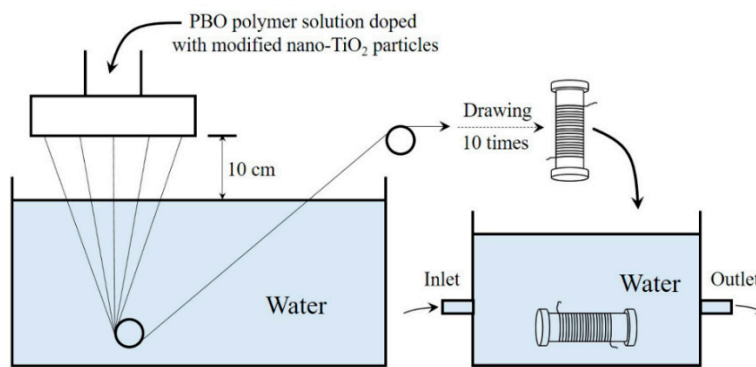


**Figure 3.** The procedure of dry-jet wet spinning of PBO fibers.

### 2.3. Characterizations and Measurements

The thermal decomposition performance of samples was determined via TG/DTG (Mettler Toledo, with a heating rate of 10 °C per minute, nitrogen atmosphere). FTIR (Bruker tensor27, Karlsruhe, Germany) was employed to characterize the chemical structure changes of modified nano-TiO<sub>2</sub> particles and PBO fibers. Furthermore, the surface morphology of nano-TiO<sub>2</sub> particles and PBO fibers were evaluated by using SEM (Hitachi S-4800, Tokyo, Japan). In addition, the UV exposure test of PBO fiber samples was carried out on a xenon lamp weatherometer (1500 W Xenon lamp, 380 nm UV rays, 250~765 W/m<sup>2</sup>). Tensile testing of fibers which were mounted on cardboard tabs was performed on the universal tensile tester (model WD-1) using two centimeter gage length at a strain rate of 2% per minute.

## 3. Results and Discussion

### 3.1. Characterizations of Modified Nano-TiO<sub>2</sub>

As Figure 1 shows, TEA causes the increase of hydroxyl ion (OH<sup>-</sup>) in the solution because of the existence of the lone pair electrons in the N atom. Owing to the high molecular polarity and high surface energy, OH<sup>-</sup> ions were adsorbed on the surface of nano-TiO<sub>2</sub> particles to form Ti(OH)<sub>n</sub>. The Ti–O bond of TDT would be hydrolyzed to the hydroxyl group (–OH) in an acid solution. The newly formed hydroxyl groups then reacted with the hydroxyl group on the surface of the TiO<sub>2</sub> to form a chemical connection. Therefore, as Figure 1 shows, the surface modifier of modified nano-TiO<sub>2</sub> was mainly from TDT.

The particle size distribution of nano-TiO<sub>2</sub> before and after modification shown in Figure 4a. The surface micromorphology of the modified nano-TiO<sub>2</sub> was evaluated via SEM shown in Figure 4b. As Figure 4b shows, the nano-TiO<sub>2</sub> particles are roughly pebble-shaped with about 50 nm in average diameter. There were many evenly distributed spots on the surface of the nano-TiO<sub>2</sub> particles, and they were caused by surface modification.

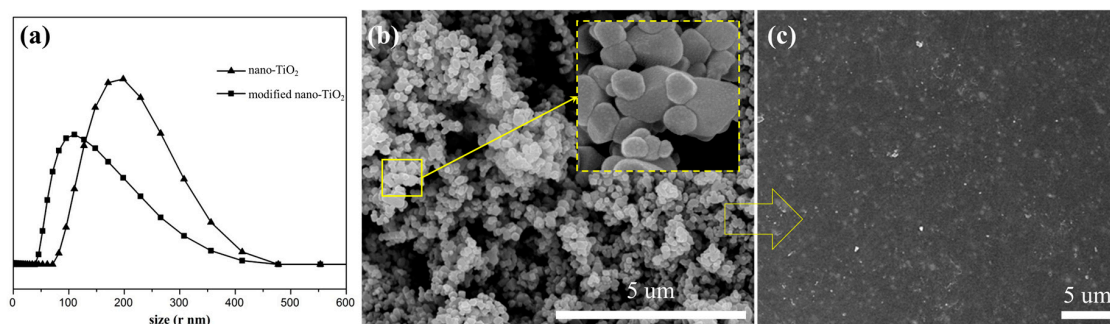


**Figure 4.** Particle size distribution of nano-TiO<sub>2</sub> before and after modification (a), SEM images of modified nano-TiO<sub>2</sub> (b), and the surface of PBO fiber containing modified nano-TiO<sub>2</sub> particles (c).

The surface modification of nano-TiO<sub>2</sub> was verified via the FTIR absorption spectra shown in Figure 5a. These spectra were used to determine the compositional changes of nano-TiO<sub>2</sub> before and after modification. A curve in Figure 5a is the FTIR spectra of pure nano-TiO<sub>2</sub>. As A curve shows, the peak at ~779 cm<sup>-1</sup> is the typical vibration of Ti–O–Ti. The broad peak at ~3420 cm<sup>-1</sup> is the typical O–H stretching vibration peak corresponding to the associated hydroxyl group of Ti(OH)<sub>n</sub>. Similarly, the peak at ~1628 cm<sup>-1</sup> is the typical H–O–H stretching vibration peak of the adsorbed water at the surface of nano-TiO<sub>2</sub> particles. After the modification of TDT, the FTIR characteristics of TDT would be reflected in the spectrum of the modified nano-TiO<sub>2</sub> (see B and C curve in Figure 5a). The peaks occurring at ~2960, 2927, and 2865 cm<sup>-1</sup> correspond to the stretching vibration of C–H. The doublet peaks at ~1461 and 1378 cm<sup>-1</sup> correspond to the bending vibration of C–H. Moreover, the peaks at ~2400, ~1229, ~1062, ~999, and ~700 cm<sup>-1</sup> are typical of TDT. The FTIR results reveal that the TDT has been successfully chemically bonded to the surface of nano-TiO<sub>2</sub> particles. TG and DTG were employed to determine the thermal performance and the content of modifier on the surface of the modified nano-TiO<sub>2</sub> particle [29], and the results were shown in Figure 5b. As can be seen from Figure 5b, the modified nano-TiO<sub>2</sub> shows continuous weight loss until about 260 °C. This can be attributed to physically adsorbed water volatilization and the thermal decomposition of modifier chains. Therefore, based on the result, the surface modifier content of nano-TiO<sub>2</sub> particles was no more than about 14 wt %.

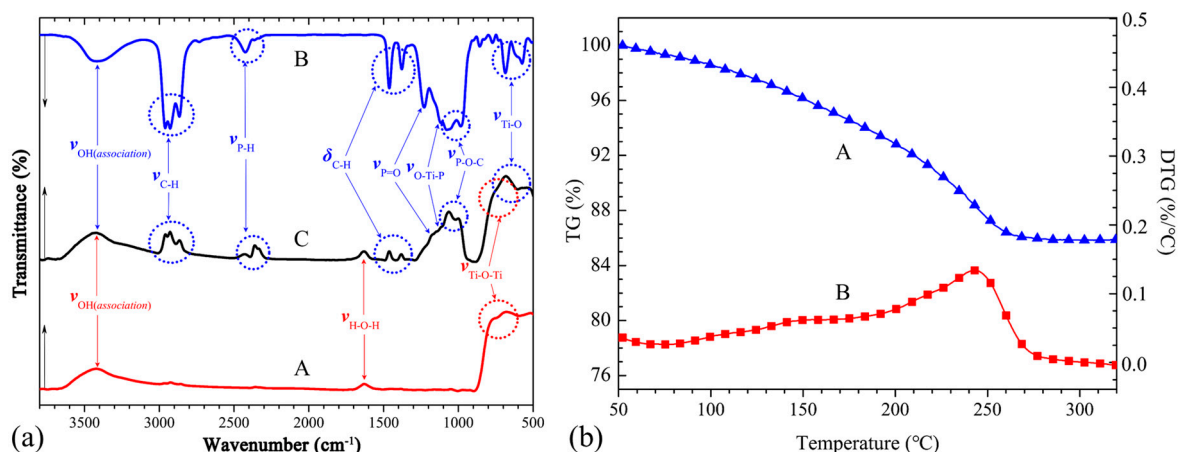


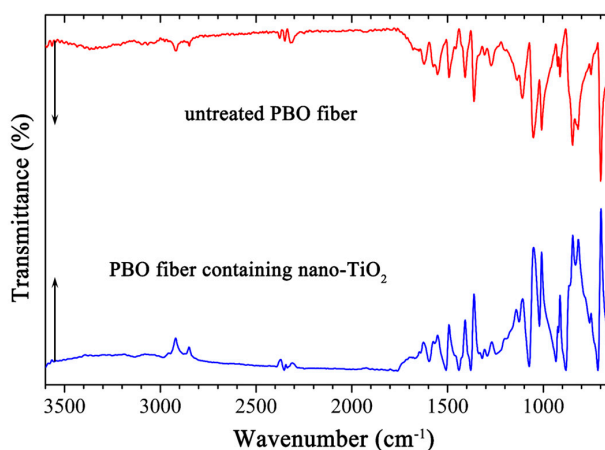
**Figure 5.** (a): FTIR spectra of pure nano-TiO<sub>2</sub> (A), tetraisopropyl di(dioctylphosphate) titanate (TDT) (B), and modified nano-TiO<sub>2</sub> (C), (b): TG (A) and derivative thermogravimetry (DTG) (B) of modified nano-TiO<sub>2</sub> under nitrogen with a heating rate of 10 °C per minute.

### 3.2. Effect of Modified Nano-TiO<sub>2</sub> on UV Aging Resistance of PBO Fiber

To investigate the effect of modified nano-TiO<sub>2</sub> on UV aging resistance of PBO fiber, the PBO fiber containing 0%, 1%, 3%, and 5% modified nano-TiO<sub>2</sub> content were prepared, and they were named PBO-0-TiO<sub>2</sub>, PBO-1-TiO<sub>2</sub>, PBO-3-TiO<sub>2</sub>, PBO-5-TiO<sub>2</sub>, respectively.

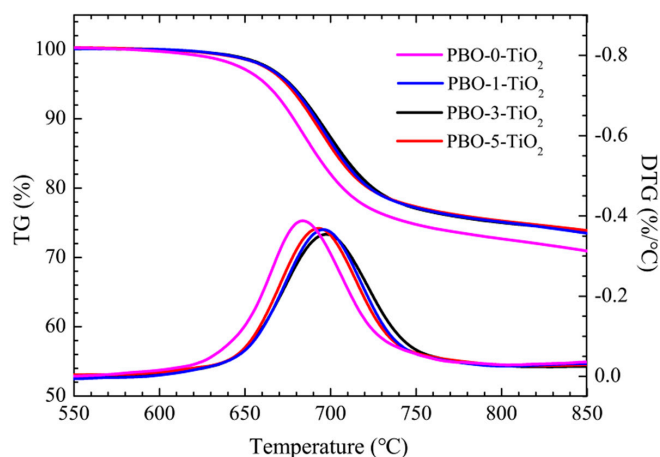
In order to investigate the relationship between the nano-TiO<sub>2</sub> content and the polymer molecular weight, the intrinsic viscosity [ $\eta$ ] values of PBO polymer solutions were determined via Ubbelohde viscometer in Methanesulfonic acid (MSA) at 30 ± 0.2 °C. The [ $\eta$ ] values of polymer solutions of PBO-0-TiO<sub>2</sub>, PBO-1-TiO<sub>2</sub>, PBO-3-TiO<sub>2</sub>, and PBO-5-TiO<sub>2</sub> were 6.0, 6.0, 5.0, and 4.0 dL/g, respectively. According to the correlation of [ $\eta$ ] and the weight-average molecular weight ( $M_w$ ) of PBO [25],  $M_w$  values of PBO-0-TiO<sub>2</sub>, PBO-1-TiO<sub>2</sub>, PBO-3-TiO<sub>2</sub>, and PBO-5-TiO<sub>2</sub> were calculated as  $2.5 \times 10^4$ ,  $2.5 \times 10^4$ ,  $2.2 \times 10^4$ , and  $1.8 \times 10^4$  g/mol, respectively. This result suggested that the molecular weight of PBO-1-TiO<sub>2</sub> was the same as PBO-0-TiO<sub>2</sub>, and as the nano-TiO<sub>2</sub> content increasing, the molecular weight of PBO polymer solution decreased gradually. This is because the incorporation of TiO<sub>2</sub> reduced the chance of PBO chain combination, which resulted in the decrease of molecular weight of PBO.

In order to investigate the effect of nano-TiO<sub>2</sub> on the morphology and composition of PBO, the surface microstructure and the chemical structure changes of PBO fiber containing 5% nano-TiO<sub>2</sub> were characterized via SEM shown in Figure 4b and via FTIR shown in Figure 6, respectively. As Figure 4b showed, the nano-TiO<sub>2</sub> embedded in the PBO matrix and even individual particles can be observed, nano-TiO<sub>2</sub> was homogeneously distributed in the PBO matrix without forming significant aggregation. As Figure 6 showed, there was no difference in the FTIR spectra between untreated PBO fiber and PBO fiber containing modified nano-TiO<sub>2</sub>. As the TiO<sub>2</sub> added, the absorption bands of modified PBO fiber were also the same as untreated PBO fiber. It means that the structure of PBO fiber was not obviously changed, and TiO<sub>2</sub> was physically dispersed in the PBO matrix and did not form a chemical connection.



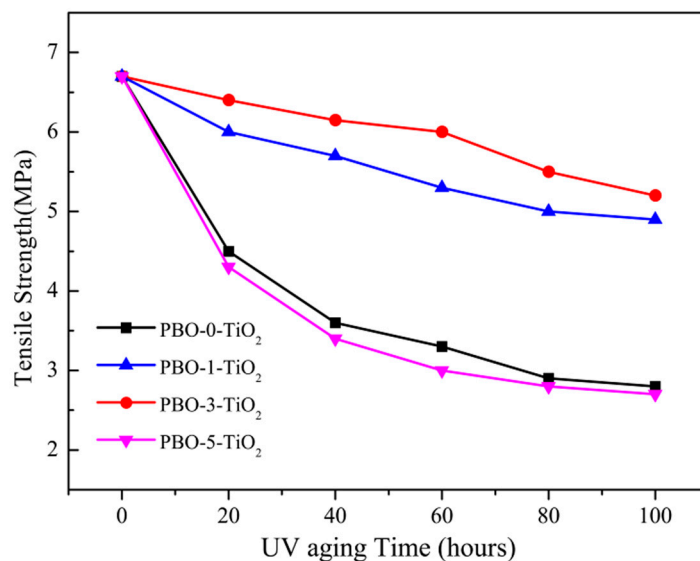
**Figure 6.** FTIR spectra of untreated PBO fiber and PBO fiber containing nano-TiO<sub>2</sub>.

TG and DTG were employed to determine the thermal performance and the effect of modified nano-TiO<sub>2</sub> on PBO fibers of PBO-0-TiO<sub>2</sub>, PBO-1-TiO<sub>2</sub>, PBO-3-TiO<sub>2</sub>, and PBO-5-TiO<sub>2</sub>, respectively. The TG and DTG results were shown in Figure 7. As Figure 7 showed, all the fibers exhibited outstanding thermal stability with no appreciable weight loss below 600 °C. The initial thermal decomposition temperature of pure PBO fiber was lower than that of PBO fibers containing modified nano-TiO<sub>2</sub>. The maximum thermal decomposition rate temperature of PBO-0-TiO<sub>2</sub>, PBO-1-TiO<sub>2</sub>, PBO-3-TiO<sub>2</sub>, and PBO-5-TiO<sub>2</sub>, was 684.2, 693.3, 696.2, and 698.1 °C, respectively. The TG and DTG results showed that nano-TiO<sub>2</sub> can help to improve the heat resistance of PBO fiber. As mentioned above, the molecular weight of PBO-0-TiO<sub>2</sub> was higher than that of the other three PBO fibers, and the molecular weight and degree of crystallinity were the main factor affecting the thermal decomposition properties of polymers. Therefore, the addition of nano-TiO<sub>2</sub> can improve the crystallinity of the PBO fibers.

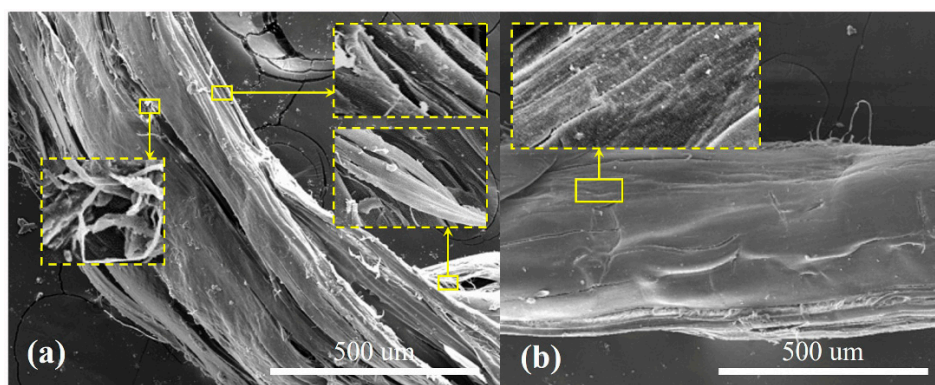


**Figure 7.** Thermogravimetric (TG) and DTG of PBO fibers under N<sub>2</sub> with a heating rate of 10 °C per minutes.

In order to investigate the effect of nano-TiO<sub>2</sub> on UV aging resistance properties of PBO fiber, the tensile strength and surface morphology of PBO fibers after UV radiation aging were characterized via universal tensile tester and SEM shown in Figures 8 and 9, respectively.



**Figure 8.** Tensile strength of the PBO fibers after UV aging for different times.



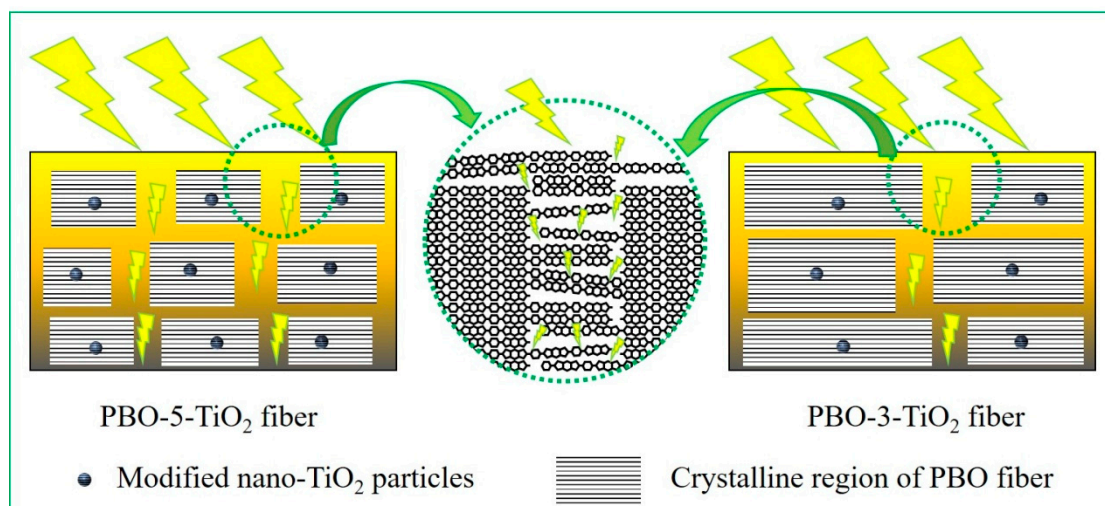
**Figure 9.** SEM images of PBO-0-TiO<sub>2</sub> fibers (a) and PBO-3-TiO<sub>2</sub> fibers (b) after exposure to UV-light for 100 h.

Figure 8 showed the relationship between the tensile strength of different PBO fibers and the exposure time of UV radiation aging. It was obvious that the nano-TiO<sub>2</sub> had a good UV protection effect on PBO fiber, and PBO-3-TiO<sub>2</sub> had the best UV aging resistance properties. The comparison of fiber morphology after aging between PBO-3-TiO<sub>2</sub> and PBO-0-TiO<sub>2</sub> was shown in Figure 9. As Figure 9 shows, after UV aging, the surface of PBO-0-TiO<sub>2</sub> fibers became rough and the cracks were obvious (see Figure 9a), while the PBO-3-TiO<sub>2</sub> fiber mainly maintained the original morphology with only slight cracks (see Figure 9b). This indicated that the nano-TiO<sub>2</sub> improved the UV aging resistance properties of PBO fiber.

Furthermore, Figure 8 results demonstrate that the tensile strengths of four PBO fibers were the same before the beginning of UV aging, and were decreased with the increase of UV aging time. Although the content of nano-TiO<sub>2</sub> in PBO-5-TiO<sub>2</sub> is higher, it is remarkable that the anti-aging properties of PBO-5-TiO<sub>2</sub> are worse than PBO-5-TiO<sub>2</sub>, even worse than PBO-0-TiO<sub>2</sub>. This indicates that the different additions of nano-TiO<sub>2</sub> have no influence on the tensile strengths of four PBO fibers without UV aging, but has a great influence on the UV anti-aging properties of PBO fiber. This result was discussed in two aspects:

Firstly, this was because the four PBO fibers had different molecular weights, chain orientations, and crystallinities. The PBO-0-TiO<sub>2</sub> has highest molecular weight, best chain orientation and least crystallinity. With the addition of nano-TiO<sub>2</sub>, the molecular weight of PBO became smaller, the molecular chain orientation became worse, but the crystallinity became higher. Therefore, with the combined effect of three factors, there was no obvious change in the strength of PBO fibers before the beginning of UV aging.

Secondly, it is worth noting that nano-TiO<sub>2</sub> could induce crystallization as a heterogeneous nucleation agent. More additive amount of nano-TiO<sub>2</sub> means more nuclei in the PBO fiber, and each single crystal region is smaller. Therefore, although PBO-3-TiO<sub>2</sub> and PBO-5-TiO<sub>2</sub> had similar crystallinity, the quantity and size of their crystal regions were different. This further means that the quantity and size of the amorphous region were different, which were the weak areas of ultraviolet aging and could be seen as the PBO fiber in a specific UV irradiation environment (see Figure 10). Therefore, although PBO-5-TiO<sub>2</sub> and PBO-3-TiO<sub>2</sub> have similar initial strength, after a period of UV aging, PBO-5-TiO<sub>2</sub> showed the worst UV aging resistance.



**Figure 10.** Schematic diagram of the influence of crystal region distribution on UV aging resistance.

#### 4. Conclusions

In this research, modified nano-TiO<sub>2</sub> was prepared by using TEA and TDT, respectively. Then the PBO fibers doped with different content modified nano-TiO<sub>2</sub> particles were prepared by preparing PBO polymer solution and dry-jet wet spinning technique. Then we studied the effect of nano-TiO<sub>2</sub> content on the properties of PBO fiber. The main conclusions of the research are as follows:

(1) TDT has a good modification effect on nano-TiO<sub>2</sub> particles, and the modified nano-TiO<sub>2</sub> particles were dispersed uniformly in the PBO matrix without forming new chemical bonds.

(2) Nano-TiO<sub>2</sub> with the addition values less than 3% could improve the anti UV aging properties of PBO fibers, while the aging resistance properties of PBO will be seriously reduced if the content of nano-TiO<sub>2</sub> is over 5%. However, nano-TiO<sub>2</sub> with the addition of no more than 5% does not affect the tensile properties of PBO fibers before the beginning of UV aging.

(3) Nano-TiO<sub>2</sub> could reduce the molecular weight and the orientation degree of PBO molecular structure and could increase the crystallinity of PBO fiber via inducing crystallization. With the increase of nano-TiO<sub>2</sub> content (over 5% content), there will be more nucleation agent and more small crystalline regions, and this will lead to more small amorphous regions and defects which are the weak regions of UV aging.

(4) Crystallinity, molecular weight and molecular chain orientation play an important role in the strength of PBO fibers before the beginning of UV aging, but for the PBO fibers irradiated with ultraviolet, the size and quantity of crystalline regions may have a more important influence.

**Author Contributions:** Conceptualization, D.W.; methodology, X.L.; software, H.W.; validation, X.L., H.W. and D.W.; formal analysis, D.W.; investigation, H.W.; resources, J.L.; data curation, X.L.; writing—original draft preparation, X.L.; writing—review and editing, J.L.; visualization, D.W.; supervision, J.L.; project administration, J.L.; funding acquisition, J.L.

**Funding:** This research received no external funding. This research did not receive any specific grant from funding agencies in the public, commercial, or not-for-profit sectors.

**Conflicts of Interest:** We declare that we have no financial and personal relationships with other people or organizations that could inappropriately influence our work, there is no professional or other personal interest of any nature or kind in any product, service or company that could be construed as influencing the position presented in, or the review of, the manuscript entitled, ‘An important factor affecting the UV aging resistance of PBO fiber doped with nano-TiO<sub>2</sub>: the number of amorphous regions’.

## References

1. Wolfe, J.F. Rigid-rod polymer synthesis: Development of mesophase polymerization in strong acid solutions. *Mat. Rec. Symp. Proc.* **1989**, *134*, 83–93. [[CrossRef](#)]
2. Martin, D.C.; Thomas, E.L. Ultrastructure of poly (para-phenylene benzobisoxazole) fibers. *Macromolecules* **1991**, *9*, 2450–2460. [[CrossRef](#)]
3. Zhu, X.L.; Zhong, W.H.; Jin, Z.M.; Zhang, P.; Guo, Z.R.; Gong, P.; Qu, Z.M. Effect of Heat-Treatment on the Properties of PBO Fibers. *Mater. Sci. Forum.* **2017**, *898*, 2107–2117. [[CrossRef](#)]
4. Xu, X.H.; Liu, X.Y.; Zhuang, Q.X.; Han, Z.W. Rigid-rod polybenzoxazoles containing perylene bisimide: Synthesis, structures and photophysical properties. *J. Appl. Polym. Sci.* **2010**, *1*, 455–460. [[CrossRef](#)]
5. Chae, H.G.; Kumar, S. Rigid-rod polymeric fibers. *J. Appl. Polym. Sci.* **2006**, *1*, 791–802. [[CrossRef](#)]
6. Shultz, A.R.; Andrady, A.L. Protection of polymers from degradation by ultraviolet light: Compensation for increased UV light intensity by increased UV absorber concentration. *J. Appl. Polym. Sci.* **2010**, *6*, 2249–2252. [[CrossRef](#)]
7. Lin, H.; Huang, Y.D.; Wang, F. Thermal stability of poly (p-phenylene benzobisoxazole) fibres. *Iran. Polym. J.* **2008**, *11*, 853–859.
8. Zhang, T.; Jin, J.H.; Yang, S.L.; Li, G.A.; Jiang, J.M. UV accelerated aging and aging resistance of dihydroxy poly(p-phenylene benzobisoxazole) fibers. *Polym. Advan. Technol.* **2011**, *5*, 743–747. [[CrossRef](#)]
9. Hu, X.D.; Jenkins, S.E.; Min, B.G.; Polk, M.B.; Kumar, S. Rigid-rod polymers: synthesis, processing, simulation, structure, and properties. *Macromol. Mater. Eng.* **2003**, *11*, 823–834. [[CrossRef](#)]
10. So, Y.H. Photodegradation mechanism and stabilization of polyphenylene oxide and rigid-rod polymers. *Polym. Int.* **2006**, *2*, 127–138. [[CrossRef](#)]
11. Song, B.; Meng, L.H.; Huang, Y.D. Enhanced UV Stability of PBO Fibers by Using Benzotriazole UV Absorber. *Key Eng. Mater.* **2012**, *522*, 931–934. [[CrossRef](#)]
12. Zhang, C.H.; Huang, Y.D.; Yuan, W.J.; Zhang, J.N. UV aging resistance properties of PBO fiber coated with nano-ZnO hybrid sizing. *J. Appl. Polym. Sci.* **2011**, *4*, 2468–2476. [[CrossRef](#)]
13. Jin, J.; Yang, S. Effects of light stabilizer on the ultraviolet stability of poly-phenylenebenzobisoxazole (PBO) fibers. *Iran. Polym. J.* **2012**, *10*, 739–745. [[CrossRef](#)]
14. Sabzi, M.; Mirabedini, S.M.; Zohuriaan-Mehr, J.; Atai, M. Surface modification of TiO<sub>2</sub> nano-particles with silane coupling agent and investigation of its effect on the properties of polyurethane composite coating. *Prog. Org. Coat.* **2009**, *2*, 222–228. [[CrossRef](#)]
15. And, T.A.; Madras, G. Photocatalytic Degradation of Rhodamine Dyes with Nano-TiO<sub>2</sub>. *Ind. Eng. Chem. Res.* **2007**, *1*, 1–7. [[CrossRef](#)]
16. Montazer, M.; Pakdel, E. Reducing Photoyellowing of Wool Using Nano TiO<sub>2</sub>. *Photochem. Photobiol.* **2010**, *2*, 255–260. [[CrossRef](#)]
17. Wang, R.M.; Wang, B.Y.; He, Y.F.; Lv, W.H.; Wang, J.F. Preparation of composited Nano-TiO<sub>2</sub> and its application on antimicrobial and self-cleaning coatings. *Polym. Advan. Technol.* **2010**, *5*, 331–336. [[CrossRef](#)]
18. Qian, D.; Dickey, E.C.; Andrews, R.; Rantell, T. Load transfer and deformation mechanisms in carbon nanotube-polystyrene composites. *Appl. Phys. Lett.* **2000**, *20*, 2868–2870. [[CrossRef](#)]
19. Liu, X.Y.; Vu, W.D.; Xu, P. Improving the photo-stability of high performance aramid fibers by sol-gel treatment. *Fiber. Polym.* **2008**, *4*, 455–460. [[CrossRef](#)]

20. Xu, L.X.; Yang, M.J. In situ compatibilization between polystyrene-grafted nano-sized TiO<sub>2</sub> and polypropylene with Friedel-Crafts catalyst. *J. Appl. Polym. Sci.* **2009**, *5*, 2755–2763. [[CrossRef](#)]
21. Zhou, C.J.; Qiu, X.Y.; Zhuang, Q.X.; Han, Z.W.; Wu, Q.L. In situ polymerization and photophysical properties of poly (p-phenylene benzobisoxazole)/multiwalled carbon nanotubes composites. *J. Appl. Polym. Sci.* **2012**, *6*, 4740–4746. [[CrossRef](#)]
22. Wu, D.C.; Shen, L.; Low, J.E.; Wong, S.Y.; Li, X.; Tjiu, W.C.; Liu, Y. Multi-walled carbon nanotube/polyimide composite film fabricated through electrophoretic deposition. *Polymer* **2010**, *10*, 2155–2160. [[CrossRef](#)]
23. Xia, B.; Li, W.; Zhang, B.; Xie, Y. Low temperature vapor-phase preparation of TiO<sub>2</sub> nanopowders. *J. Mater. Sci.* **1999**, *14*, 3505–3511. [[CrossRef](#)]
24. Sun, Q.F.; Lu, Y.; Zhang, H.M.; Zhao, H.J.; Yu, H.P.; Xu, J.S.; Fu, Y.C.; Yang, D.J.; Liu, Y.X. Hydrothermal fabrication of rutile TiO<sub>2</sub> submicrospheres on wood surface: An efficient method to prepare UV-protective wood. *Mater. Chem. Phys.* **2012**, *1*, 253–258. [[CrossRef](#)]
25. Hu, Z.; Huang, Y.D.; Wang, F.; Yao, Y.H.; Sun, S.F.; Li, Y.W.; Jiang, Z.X.; Xu, H.F.; Tang, P.Y. Synthesis of novel single-walled carbon nanotubes/poly (p-phenylene benzobisoxazole) nanocomposite. *Polym. Bull.* **2011**, *9*, 1731–1739. [[CrossRef](#)]
26. Imai, Y.; Itoya, K.; Kakimoto, M. Synthesis of aromatic polybenzoxazoles by silylation method and their thermal and mechanical properties. *Macromol. Chem. Phys.* **2000**, *17*, 2251–2256. [[CrossRef](#)]
27. Özaytekin, I.; Karatas, I. Synthesis and properties of poly (benzoxazole)s prepared from aromatic dihydroxamoyl chlorides. *High. Perform. Polym.* **2008**, *6*, 615–626. [[CrossRef](#)]
28. Kim, Y.J.; Einsla, B.R.; Tchatchoua, C.N.; McGrath, J.E. Synthesis of high molecular weight polybenzoxazoles in polyphosphoric acid and investigation of their hydrolytic stability under acidic conditions. *High. Perform. Polym.* **2005**, *3*, 377–401. [[CrossRef](#)]
29. Hsu, S.L.C.; Chang, K.C. Synthesis and properties of polybenzoxazole-clay nanocomposites. *Polymer* **2002**, *15*, 4097–4101. [[CrossRef](#)]



© 2019 by the authors. Licensee MDPI, Basel, Switzerland. This article is an open access article distributed under the terms and conditions of the Creative Commons Attribution (CC BY) license (<http://creativecommons.org/licenses/by/4.0/>).